Reprinted from
Jpn. J. Appl. Phys. Vol. 40 (2001) pp. 5187–5193
Part 1, No. 8, August 2001
©2001 The Japan Society of Applied Physics

Range-Modulated Pencil Beam Algorithm for Proton Dose Calculations

Ryosuke KOHNO, Yoshihisa TAKADA, Takeji SAKAE[1], Akihiro NOHTOMI, Toshiyuki TERUNUMA[2], Keiji MATSUMOTO and Hiroyuki MATSUDA

Institute of Applied Physics, University of Tsukuba, Tsukuba 305-8573, Japan
[1]*Institute of Clinical Medicine, University of Tsukuba, Tsukuba 305-8575, Japan*
[2]*Proton Medical Research Center, University of Tsukuba, Tsukuba 305-8575, Japan*

Jpn. J. Appl. Phys. Vol. 40 (2001) pp. 5187–5193
Part 1, No. 8, August 2001
©2001 The Japan Society of Applied Physics

Range-Modulated Pencil Beam Algorithm for Proton Dose Calculations

Ryosuke KOHNO*, Yoshihisa TAKADA, Takeji SAKAE[1], Akihiro NOHTOMI, Toshiyuki TERUNUMA[2], Keiji MATSUMOTO and Hiroyuki MATSUDA

Institute of Applied Physics, University of Tsukuba, Tsukuba 305-8573, Japan
[1]*Institute of Clinical Medicine, University of Tsukuba, Tsukuba 305-8575, Japan*
[2]*Proton Medical Research Center, University of Tsukuba, Tsukuba 305-8575, Japan*

(Received March 5, 2001; accepted for publication May 17, 2001)

The range-modulated pencil beam algorithm (RMPBA) has been developed for proton treatment planning on the basis of the pencil beam algorithm (PBA) to reduce the calculation time yet realize sufficient accuracy. It uses the depth-dose distribution of the range-modulated beam as a central-axis term of pencil beams. The spread of the range-modulated pencil beam is derived by assuming that the protons pass through the average thickness of the ridge-filter. The accuracy of dose calculations by the RMPBA is verified by comparison with dose measurements in water performed using a silicon semiconductor detector. The results of the measured dose distributions agree well with those of the calculations using the RMPBA. Furthermore, the calculation time required by the RMPBA is one-sixth of that required by the PBA in the case of the six-step ridge-filter. Therefore, the dose-calculation method by the RMPBA will be useful and applicable to actual treatment planning of proton therapy.

KEYWORDS: range-modulated pencil beam algorithm, pencil beam algorithm, ridge-filter, range-modulated proton beam, proton dose distribution

1. Introduction

A proton dose-calculation method using the broad-beam algorithm (BBA)[1–3] has been widely used for treatment planning because of its simplicity and short calculation time. However, the calculation results often do not agree well with the measurement results for a target with large lateral heterogeneities since it does not take into account the effect of ray mixing by multiple scattering effects of protons[4] in materials.

To improve accuracy, dose-calculation methods based on the pencil beam algorithm (PBA) have been developed.[1–3,5,6] In the previous paper[2] we reported the results of experimental evaluation of the PBA. Calculated results by the PBA agreed well with the measured dose distributions formed by the unmodulated proton beam traversing an L-shaped phantom within the rms error of 2.3% and the calculation time required by the PBA was relatively short. It is suggested that the dose-calculation method by the PBA will be useful and applicable to actual treatment planning of proton therapy.

In actual proton therapy, most patients are treated by range-modulated proton beams using a range modulator such as a ridge-filter or a rotating wheel.[7,8] For such beams, Hong *et al.* reported that the depth-dose distribution by the PBA agreed well with the experimental result.[1] Petti also evaluated the usefulness of the PBA by the comparison between the results of the PBA and Monte Carlo calculation and verified that the dose calculations by the PBA gave reasonably accurate results.[3] On the other hand, for range-modulated proton beams, we usually have to calculate the dose contributions of pencil beams traversing the individual elements of the ridge-filter and sum them up to obtain the dose distribution. Since the number of elements of the ridge-filter typically amounts to about ten to twenty, the required calculation time is relatively large.

In this paper, we propose a range-modulated pencil beam algorithm (RMPBA) which improves the dose-calculation time yet is sufficiently accurate. The usefulness of dose calculation by the RMPBA for a range-modulated proton beam is verified by comparison between the results of measurements and calculations by the PBA.

2. Dose Calculation Algorithm

2.1 Pencil beam algorithm

Hong *et al.* have already developed a method of dose calculation based on the PBA.[1] Hong's PBA considered the effective source with Gaussian spatial distribution and uniform angular distribution at the effective source point and applied the depth-dose distribution of the "open beam" to the central-axis term. Here, since they define the open beam as a proton beam free of any beam-modifying devices other than those which are always in the beam, the open beam excludes a fine degrader. We modified Hong's method as follows:[2] (1) We considered the effective source as that with a Gaussian intensity profile and a Gaussian angular distribution. (2) We used the depth-dose distribution of the unmodulated broad beam passing through a fine degrader and always required devices, the scatterer and the monitoring devices, in the beam line as the central-axis term of pencil beams. This means that we can omit calculation of the behavior of proton beams in a fine degrader.

In our PBA, the beam can be assumed to be emitted from an effective source point which is characterized by an upright phase space ellipse. The phase space parameters can be calculated by integrating the scattering in slabs as follows:[2] The square of proton beam size at depth, z, after passing through slabs is given by

$$\sigma_{11}(z) = \sigma_{11,0} + 2\sigma_{12,0}z + \sigma_{22,0}z^2 + \int_0^z (z-s)^2 \frac{d\bar{\theta^2}}{ds} ds, \quad (1)$$

$$\sqrt{\bar{\theta^2}} = \frac{14.1}{p\beta c}\sqrt{\frac{z}{L_r}}\left(1 + \frac{1}{9}\log_{10}\frac{z}{L_r}\right). \quad (2)$$

Equation (2) is termed the Highland Formula,[4,9] where σ_{11},

*E-mail address: kohno@pmrc.tsukuba.ac.jp

σ_{12} and σ_{22} are components of the σ-matrix expressing the phase space parameters at a longitudinal position z, $\sqrt{\bar{\theta}^2}$ the rms of the distribution of the projection angle in a plane extended by the beam axis and the horizontal axis, p the proton momentum in units of MeV/c and βc the velocity of a proton. L_r is the radiation length of the material in units of g/cm^2. $p\beta c$ is calculated in advance as a function of the proton range. The components of σ-matrix with an additional index 0 are those at an initial point of calculation. By this method, we can determine accurately and simply the behavior of a proton beam in materials.

In this paper, furthermore, we calculate dose distributions for a range-modulated beam. A range-modulated beam for which the width of the Bragg-peak dose region is spread out can be accomplished in a bar ridge-filter in a stepwise manner.[7,8] It is made of aluminum and has ridge-filter elements in a stepwise manner, which changes beam weights and beam energies, so that the resulting Bragg peaks are stacked throughout the depth of the target volume.

The dose $F(x, y, z; (x_0, y_0))$ by a single pencil beam with entrance position, (x_0, y_0), is given by

$$F(x, y, z; (x_0, y_0)) = \phi(x_0, y_0) w(i) DD(z + z_r(i)) \frac{1}{2\pi\sigma(z + z_r(i))^2} \times \exp\left(-\frac{(x_0 - x)^2 + (y_0 - y)^2}{2\sigma(z + z_r(i))^2}\right), \quad (3)$$

where $\phi(x_0, y_0)$ is the measured intensity profile of the unmodulated broad beam at the entrance position of the target, $w(i)$ the beam weight in an i-th ridge-filter element, $DD(z + 0)$ the depth-dose distribution of the broad beam in the case that the ridge-filter is removed and $z_r(i)$ is the range loss in an i-th ridge-filter element. Here, we convert $\sigma_{11}(z)$ in eq. (1) to $\sigma(z + z_r(i))^2$.

2.2 *Range-modulated pencil beam algorithm*

We developed the RMPBA on the basis of the PBA to reduce the calculation time yet realize sufficient accuracy. Figure 1 depicts simply the difference of dose calculation methods between the PBA (a) and the RMPBA (b). As Fig. 1(a) indicates, in the PBA, we have to calculate dose contributions of pencil beams traversing the individual elements of the ridge-filter in a stepwise manner and sum them up to obtain the dose distribution by the range-modulated beam. In other words, we have to calculate proton energy losses, beam weights and phase space parameters for each ridge-filter element. This is a relatively time-consuming task. As an improvement, the RMPBA has been developed. In the case of Fig. 1, although a range-modulated broad beam is formed by pencil beams passing through three elements of the ridge-filter, as shown in Fig. 1(b), we assumed that it was formed by a set of each range-modulated pencil beam traversing the "assumed ridge-filter" with the average thickness of the ridge-filter as well as the fundamental concept of the pencil beam algorithm. That is to say, the RMPBA substitutes the single range-modulated pencil beam drawn in Fig. 1(b) for three unmodulated pencil beams traversing the individual ridge-filter elements in Fig. 1(a) so that the RMPBA can accomplish the reduction of dose calculation time.

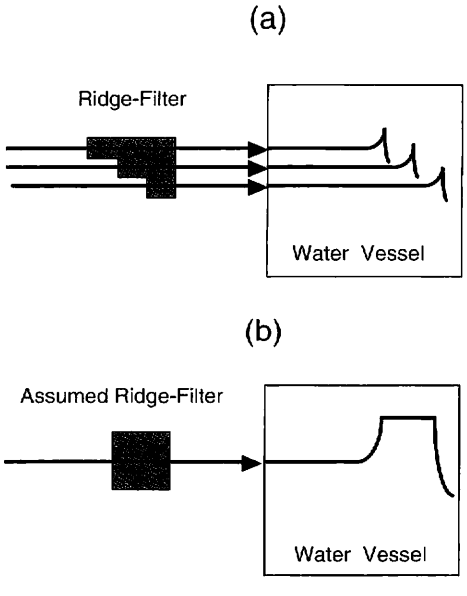

Fig. 1. The difference of the concepts for dose calculation method between the conventional PBA (a) and the RMPBA (b).

The dose $F(x, y, z; (x_0, y_0))$ generated by a single range-modulated pencil beam is given by

$$F(x, y, z; (x_0, y_0)) = \phi(x_0, y_0) RMDD(z) \frac{1}{2\pi\sigma(z)^2} \times \exp\left(-\frac{(x_0 - x)^2 + (y_0 - y)^2}{2\sigma(z)^2}\right), \quad (4)$$

where $RMDD(z)$ is obtained by fitting the measured depth-dose distribution of the range-modulated broad beam with a number of concatenated polynomial functions. Since $RMDD(z)$ necessarily includes range-straggling effects and nuclear interactions in instruments of a beam line, the depth-dose distribution by the RMPBA should reproduce the experimental result more accurately than that by the PBA. Using eq. (1), we derived the spread of the range-modulated pencil beam, $\sigma(z)$ in eq. (4), by assuming that the protons passed through the assumed ridge-filter. In this way, a range-modulated pencil beam can be treated as a whole, which serves to simplify the calculation.

3. Experimental Arrangement

Measurements were carried out using the horizontal beam line at the Proton Medical Research Center (PMRC), University of Tsukuba. Approximately monoenergetic 250 MeV protons are supplied from the KEK 500 MeV booster synchrotron through a carbon energy-degrader and a momentum-analyzing system of the medical beam line.[10] Since the beam energy is degraded heavily in the carbon degrader, the energy straggling becomes large and momentum spread of trans-

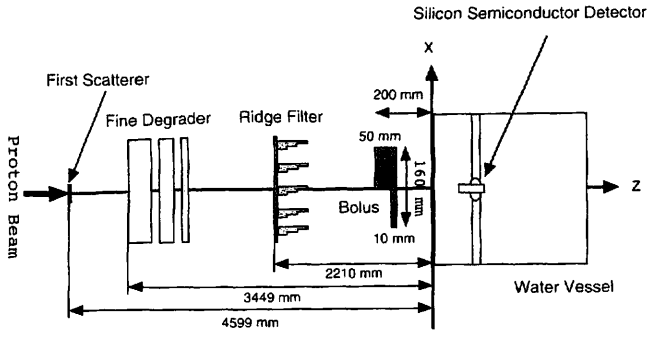

Fig. 2. Experimental arrangement for measurements of dose distributions in water (plan view).

ported beam is as large as ±1.3%, which results in the large distal fall-off (80–20% distal fall-off = 13 mm) of the obtained Bragg curves.

The experimental arrangement is sketched in Fig. 2 (plan view). The incident protons were scattered by a 3-mm-thick lead plate (referred to as "the first scatterer") to obtain a laterally uniform spatial distribution at the measurement position. A binary range shifter ["fine degrader" (FD)] and a ridge-filter (RF) were placed between the first scatterer and the patient couch on which we mounted the measurement devices of dose distribution.

We prepared a bolus with an L-shaped horizontal cross section made of Mix-DP, which is a tissue-equivalent material for X-rays. The thinner part, $x < 0$, of the bolus measured 10 mm and the thicker part, $x \geq 0$, measured 50 mm. There was no structure in the y-direction and the height was 100 mm. It had an abrupt change of thickness in the lateral direction. This bolus shape was selected to obtain a target with large heterogeneity in the lateral direction. The origin of the y-coordinate was defined at the middle of the bolus. A silicon semiconductor detector (SSD) was set at $y = 0$ in this experiment.

4. Measurements of Dose Distributions

For modulated proton beams, the depth (z)-dose distributions were measured by moving the SSD in the z-direction at $x = -40$ mm in water and the lateral (x)-dose distributions were measured in the region of interest at intervals of 5 mm in water as follows: (1) We inserted a fine degrader of 120 mm and a ridge-filter of 40 mm "spread-out Bragg peak (SOBP)" width, (FD, RF) = (120, 40), in the beam line. The average energy of the beam traversing them was 178 MeV. (2) We inserted (FD, RF) = (240, 40). The average energy was 103 MeV. The reason why we selected two kinds of energies is that we could verify the estimation of the beam spread by the RMPBA for both high and low energy proton beams. In particular, since a low energy proton beam has a large angular spread, the calculated beam spread using the average proton energy by the RMPBA may have a larger error.

5. Results and Discussion

The measured dose distributions are compared with calculated ones based on the RMPBA and the PBA. In the calculation by the RMPBA, the angular spread of the range-modulated pencil beam parameter, $\sqrt{\sigma_{22,0}}$, was determined by measuring the beam profile of protons passing through the first scatterer, fine degrader (FD = 120 or 240 mm) and a ridge-filter (RF = 40 mm) in the beam line and a block collimator with a small circular hole, at five different positions downstream of the collimator and by fitting the profile data with the second polynomial equation. The obtained values for (FD, RF) = (120, 40) and (240, 40) are 0.0099 ± 0.0016 (1 s.d.) and 0.012 ± 0.003 rad, respectively, under the assumption that $\sigma_{11,0}$ and $\sigma_{12,0}$ are 0. Since the effective source point is far from the measurement position and the region of interest is around the origin, we assumed that the beam was a parallel beam. Parallel pencil beams were generated with a lateral pitch of 0.5 mm at the entrance surface of the bolus $z = -200$ mm. The lateral pitch was selected so that a finer pitch did not produce any difference in the calculation results. We took a relative dose of 100% at $(x, z) = (-40, 175)$, which is the center of the SOBP, in the case of (FD, RF) = (120, 40) and that at $(-40, 55)$ in the case of (FD, RF) = (240, 40).

On the other hand, in the PBA, the beam angular parameters in FD = 120 and 240 at the entrance surface of the ridge-filter were 0.009 and 0.011 rad. The only beam angular parameters of pencil beams traversing the individual elements of the ridge-filter are calculated from the entrance surface of the ridge-filter to $z = -200$ mm and we regard the obtained values as the $\sqrt{\sigma_{22,0}}$ parameters for each ridge-filter element at $z = -200$ mm. Using these parameters, the PBA as well as the RMPBA values were calculated. In order to clarify the different contributions of the off-axis term to the dose between the PBA and the RMPBA, we took the central-axis term of the PBA to be the same as that of the RMPBA as follows:

$$\sum_i w(i) DD(z + z_r(i)) RMDD(z).$$

Figures 3 and 4 show the measured depth (z)-dose distributions at $x = -40$ mm in (FD, RF) = (120, 40) and (240, 40) along with the calculations. Depth-dose distributions by the RMPBA agree well with the measured ones within the acceptable range of measurement error, about 1.5%, of the measured dose due to beam fluctuation.

Figures 5 and 6 depict lateral spread of proton beams at

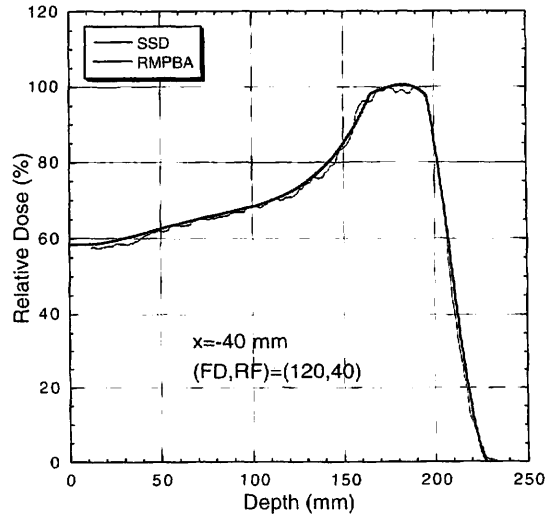

Fig. 3. Comparison between the depth-dose distribution by the measurement with the SSD (fine solid line) and that by calculation based on the RMPBA (bold solid line) at $x = -40$ mm in water for the case of (FD, RF) = (120, 40).

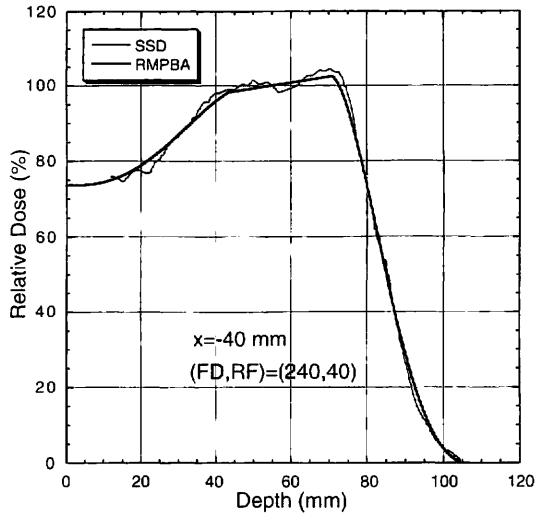

Fig. 4. Comparison between the depth-dose distribution by the measurements with the SSD (fine solid line) and that by calculation based on the RMPBA (bold solid line) at $x = -40$ mm in water for the case of (FD, RF) = (240, 40).

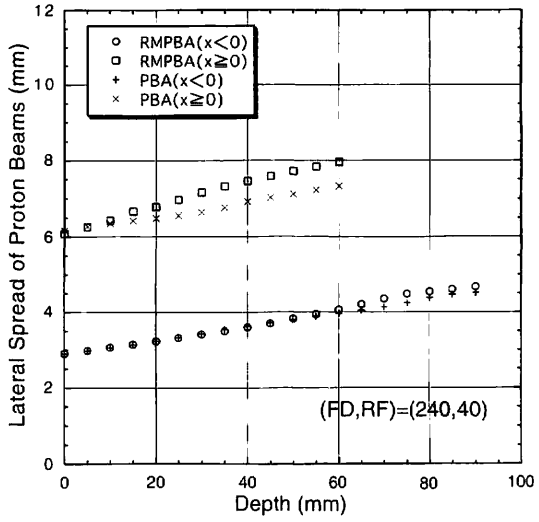

Fig. 6. Comparison between the lateral spread of proton beams at $x < 0$ and $x \geq 0$ by the RMPBA and that by the PBA in water for the case of (FD, RF) = (240, 40).

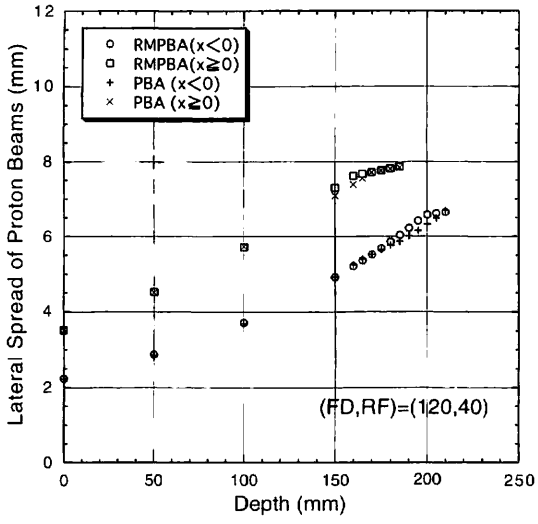

Fig. 5. Comparison between the lateral spread of proton beams at $x < 0$ and $x \geq 0$ by the RMPBA and that by the PBA in water for the case of (FD, RF) = (120, 40).

$x < 0$ and $x \geq 0$ by the RMPBA and the PBA for the two cases of (FD, RF) = (120, 40) and (240, 40), respectively. In the PBA, the lateral spread, $\sigma(z)$, of proton beams was derived in the following way: Contributions of individual pencil beams passing through parts of various thicknesses in the ridge-filter were calculated and summed up to obtain a lateral dose distribution in the specified depth. Then the distribution was fitted by a Gaussian function to obtain the lateral spread, $\sigma(z)$. The coincidence between the results of both the RMPBA and the PBA is perfect in the shallower region before the proximal end of the SOBP since all protons penetrating through regions of various thicknesses of the ridge-filter contribute to the dose distribution. On the other hand, some differences can be noticed in the deeper region behind the proximal end of the SOBP since a portion of protons traversing the thicker part of a ridge-filter stops before the depth of interest. Therefore the RMPBA generally overestimates the lateral spread in the deeper region of the SOBP curve. In addition, the lateral spread of the beam consists of two components: one is due to the angular spread of the incident beam and the other is due to the scattering in the phantom and water. Since the latter component overrides the former in a deeper region, the differences of the lateral spread between the PBA and the RMPBA are relatively small for both the cases in Fig. 5 and the $x < 0$ case in Fig. 6. On the other hand, since the former component contributes more to the lateral spread for the $x \geq 0$ case in Fig. 6, a larger difference of the lateral spread is noticed. However, the difference is small compared with the lateral spread itself.

Figures 7(a)–7(c) and 8(a)–8(c) are, respectively, measured lateral (x)-dose distributions at $z = 160$, 180, 200 mm in the case of (FD, RF) = (120, 40) and at $z = 35$, 55, 75 mm in the case of (FD, RF) = (240, 40) together with the calculations. We found that, in all cases, the dose distributions by the RMPBA coincide well with those by the PBA. This means that both differences in Figs. 5 and 6 do not affect dose distributions much. Here, we studied the effect of measurement error of angular spread, $\sqrt{\sigma_{22,0}}$, on the lateral distributions. For that purpose, we evaluated the contribution of $\sigma_{22,0}$ measurement error to lateral $\sigma(z)$ calculations. We found that maximum change of lateral penumbra (80–20%) by $\sqrt{\sigma_{22,0}}$ measurement errors in the RMPBA was less than about 0.8 mm.

Figures 9(a)–9(c), 10(a)–10(c) show iso-dose distributions obtained by the measurements, calculations by the RMPBA as well as those by the PBA in the cases of (FD, RF) = (120, 40) and (240, 40), respectively. The iso-dose curves are drawn for every 10% increase of the relative dose. Figures 8(a) and 9(a) are obtained by interpolating the experimental lateral-dose distributions taken in 5 mm steps in the depth direction. The white region shows that with a dose of more than 90% of the maximum and the black region that with a dose of less than 10% of the maximum. These figures show that the iso-dose distributions by the RMPBA and the PBA agree well with the experimental results.

The calculation time required by the RMPBA is much shorter than that by the PBA. The reduction factor depends

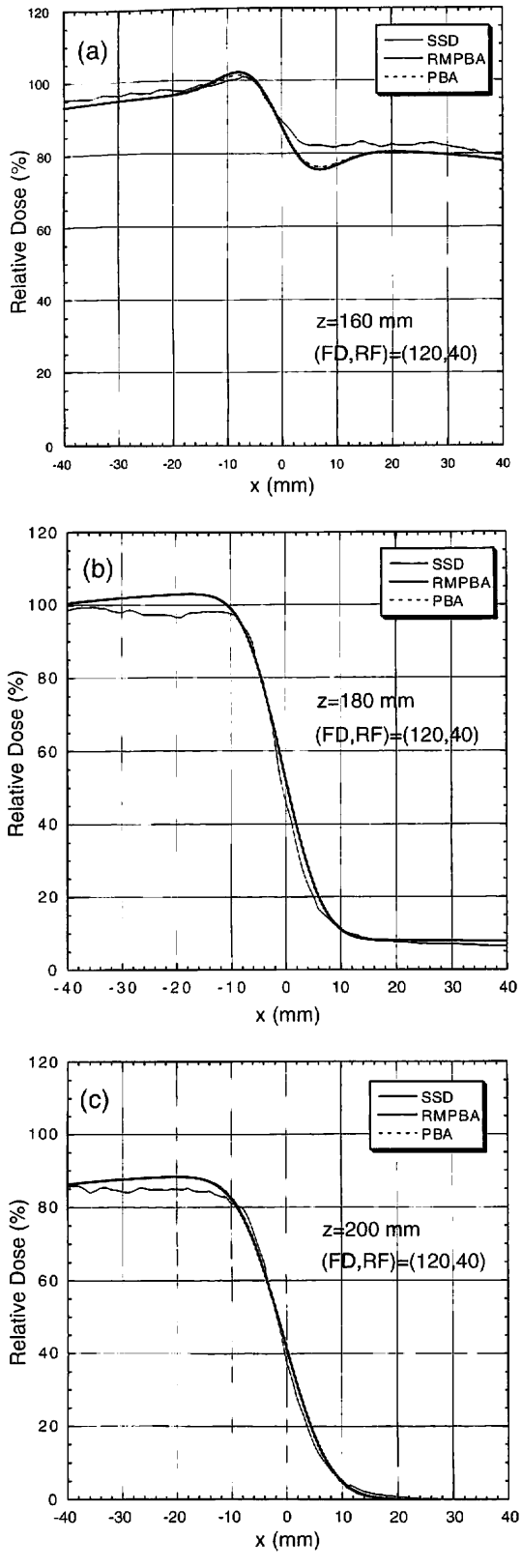

Fig. 7. Comparison among the lateral-dose distributions by the measurements with the SSD (fine solid line), those by calculations based on the RMPBA (bold solid line) and those by calculations based on the PBA (dotted line) at z = 160 (a), 180 (b) and 200 mm (c) in water for the case of (FD, RF) = (120, 40).

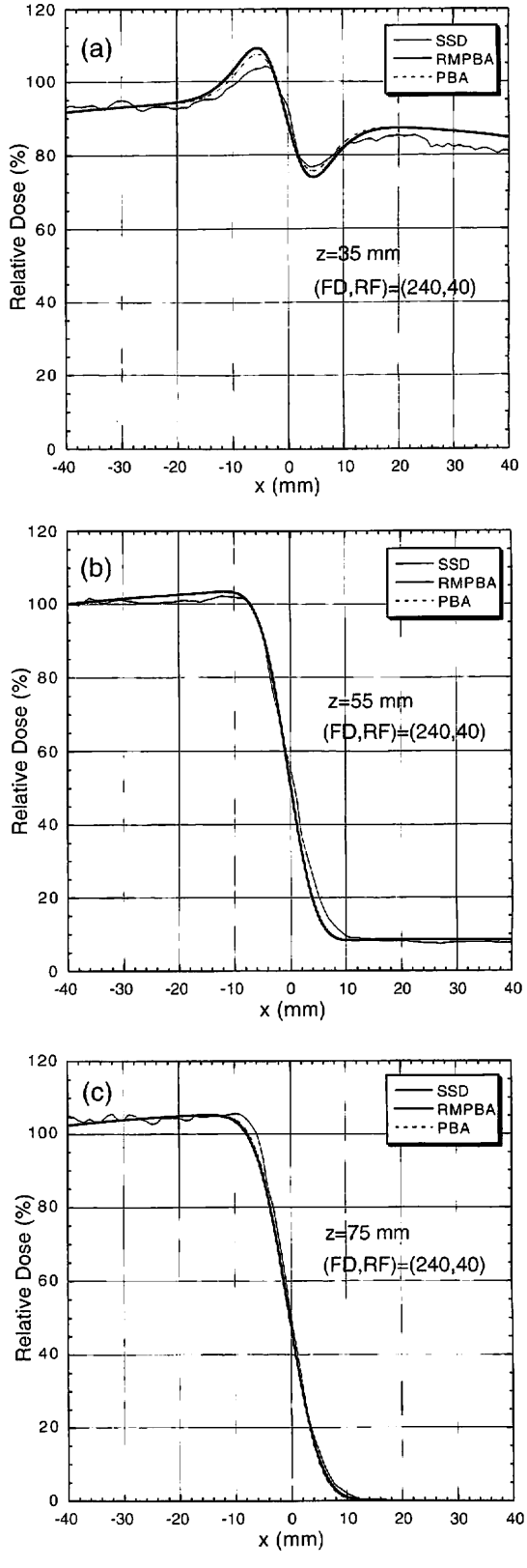

Fig. 8. Comparison among the lateral-dose distributions by the measurements with the SSD (fine solid line), those by calculations based on the RMPBA (bold solid line) and those by calculations based on the PBA (dotted line) at z = 35 (a), 55 (b) and 75 mm (C) in water for the case of (FD, RF) = (240, 40).

on the number of steps of the ridge-filter. Since the number of the ridge-filter steps is six in the present case, the reduction factor was one-sixth. As the number of the ridge-filter steps amounts to about ten to twenty for a good quality beam, one order of reduction can be expected in typical cases.

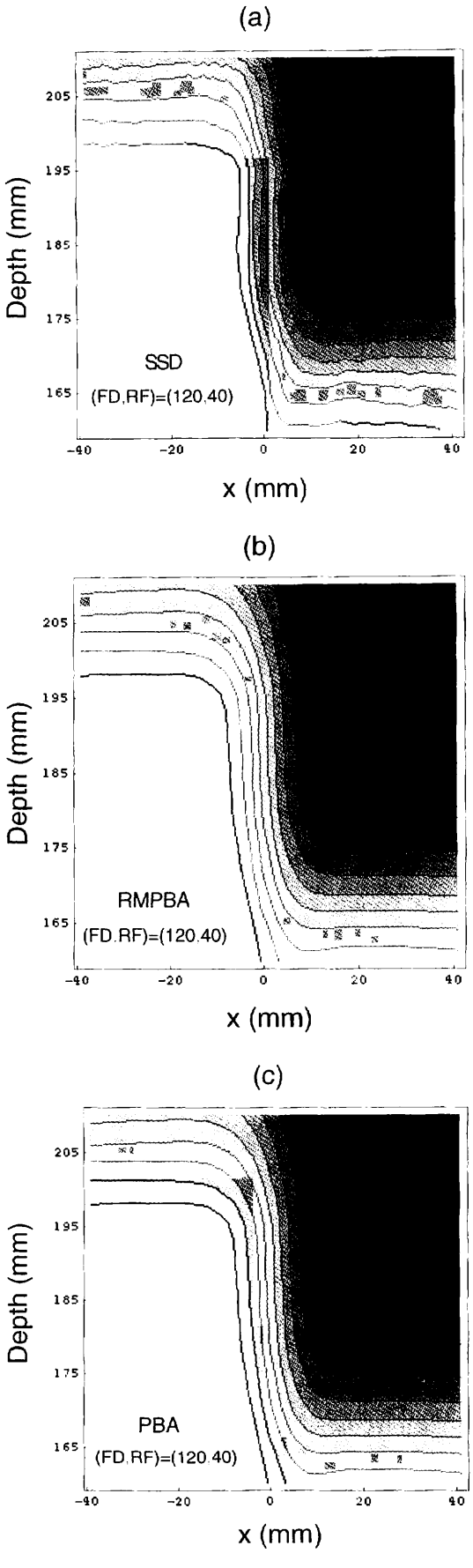

Fig. 9. Comparison among the iso-dose distributions drawn for every 10% of the relative dose by the measurements with the SSD (a), that by calculation based on the RMPBA (b) and that by calculation based on the PBA(c) in water for the case of (FD, RF) = (120, 40).

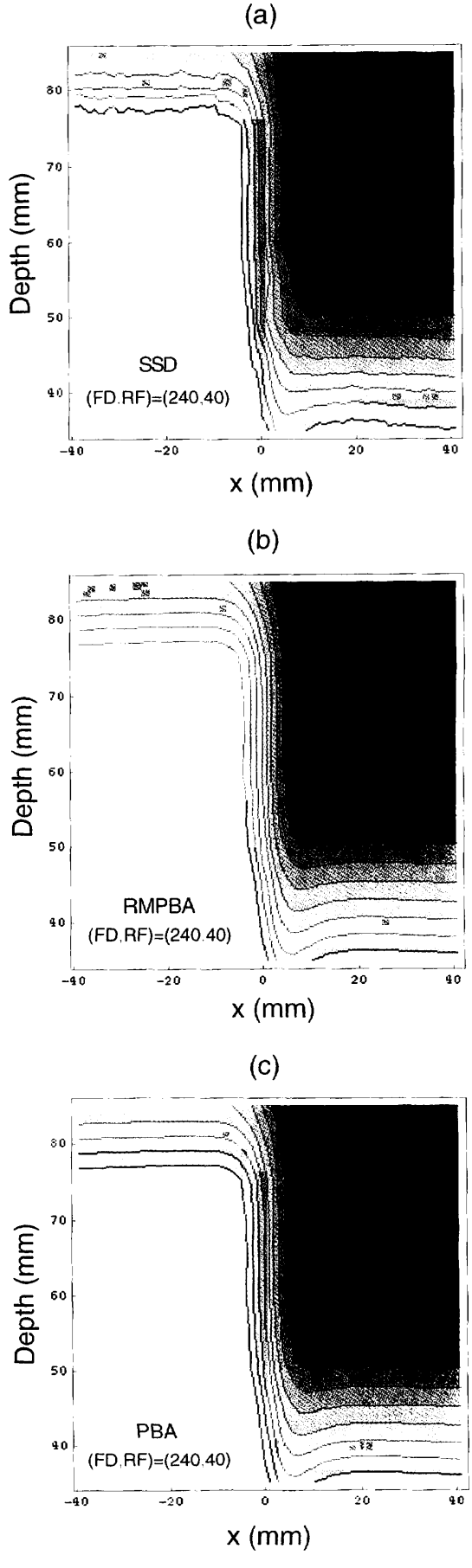

Fig. 10. Comparison among the iso-dose distributions drawn for every 10% of the relative dose by the measurements with the SSD (a), that by calculation based on the RMPBA (b) and that by calculation based on the PBA (c) in water for the case of (FD, RF) = (240, 40).

6. Conclusions

Dose calculations by the RMPBA, in which measured depth-dose curve of modulated beam, $RMDD(z)$, and measured angular spread, $\sigma_{22,0}$, of the incident beam are used, agree well with the measurement results. Furthermore, we can achieve a significant reduction of calculation time, one order of magnitude, in typical cases. It is feasible to use the RMPBA for the dose calculation for proton treatment planning for most targets.

1) L. Hong, M. Goiten, M. Bucciolini, R. Comiskey, B. Gottscalk, S. Rosenthal, C. Serago and M. Urie: Phys. Med. Biol. **41** (1996) 1305.
2) R. Kohno, Y. Takada, T. Sakae, A. Nohtomi, T. Terunuma and K. Yasuoka: Jpn. J. Appl. Phys. **40** (2001) 441.
3) P. L. Petti: Med. Phys. **19** (1992) 137.
4) B. Gottscalk, A. M. Koehler, R. J. Schneider, J. M. Sisterson and M. S. Wagner: Nucl. Instrum. & Methods B **74** (1993) 467.
5) A. K. Carlsson, P. Andreo and A. Brahme: Phys. Med. Biol. **42** (1997) 1033.
6) B. Schaffner, E. Pedroni and A. Lomax: Phys. Med. Biol. **44** (1999) 27.
7) A. M. Koehler, R. J. Schneider and J. M. Sisterson: Nucl. Instrum. & Methods **131** (1975) 437.
8) W. T. Chu, B. A. Ludewigt and T. R. Renner: *Instrumentation for Treatment of Cancer Using Proton and Light-Ion Beams* (Lawrence Berkeley Laboratory, Univ. of California, Berkeley, CA 94720, 1993) p. 49.
9) V. L. Highland: Nucl. Instrum. & Methods **129** (1975) 497.
10) D. Kurihara, S. Suwa, A. Tachikawa, Y. Takada and K. Takikawa: Jpn. J. Appl. Phys. **22** (1983) 1599.